European Journal of Pharmaceutical Sciences 49 (2013) 723–731

Contents lists available at SciVerse ScienceDirect

European Journal of Pharmaceutical Sciences

journal homepage: www.elsevier.com/locate/ejps

Investigation and correlation of physical stability, dissolution behaviour and interaction parameter of amorphous solid dispersions of telmisartan: A drug development perspective

R. Dukeck, P. Sieger, P. Karmwar *

Department of Drug Discovery Support, Boehringer-Ingelheim Pharma GmbH & Co. KG, Biberach an der Riss 88397, Germany

ARTICLE INFO

Article history:
Received 28 February 2013
Received in revised form 22 April 2013
Accepted 3 May 2013
Available online 16 May 2013

Keywords:
Amorphous
Stability
Dissolution
Drug–polymer interaction
Solid dispersions
Telmisartan

ABSTRACT

The aim of this study was to investigate if amorphous solid dispersions of telmisartan, prepared in presence of different polymers, exhibit different structural and thermodynamic characteristics and whether these differences can be correlated to their physical stability (time to crystallisation) and dissolution behaviour. Amorphous samples were prepared by melt quenching. The resulting amorphous materials were characterised using X-ray diffraction, Raman spectroscopy and differential scanning calorimetry. All freshly prepared samples were completely X-ray amorphous (with a halo being the only feature in the diffractograms). The shape of the halos in the diffractograms varied suggesting structural variations in the near order of the molecules between the different amorphous solid dispersions (ASDs). Principal component analysis of the Raman spectra of the various ASD revealed that the samples clustered in the scores plot, again suggesting structural differences due to the presence of different drug–polymer interaction. The ranking of the samples with respect to physical stability and interaction parameter was: ASD of telmisartan:eudragit > ASD of telmisartan:soluplus > ASD of telmisartan:HPMC > ASD of telmisartan:PVP > amorphous telmisartan. The interaction parameter, calculated by using the Flory Huggins theory, showed a good correlation with the experimentally determined stability whereas a weak correlation was found with dissolution behaviour of different ASD. This study showed that correlation of physical stability and dissolution behaviour with calculated interaction parameter is possible for the same amorphous systems prepared by using different polymers. This could aid in selecting the most appropriate polymer for the development of optimised formulations containing amorphous drugs. It can be concluded that ASD prepared by using different polymers have different structural and thermal properties. These differences affect the physical stability and dissolution profiles of the amorphous solids. Thus, choosing the right polymer for preparing ASD is critical for producing materials with desired dissolution profiles and enhanced stability.

1. Introduction

Many new chemical entities coming out of pharmaceutical drug discovery exhibit low aqueous solubility and subsequently poor bioavailability after oral administration (BCS class 2 drugs) (Patterson et al., 2007). It is therefore often required to enhance dissolution rate and solubility of these compounds, to allow the further development of a drug into a medicine.

From a formulation point of view, particularly BCS Class II drugs with poor solubility but high permeability comprise an interesting development platform, since formulation strategies may be applied to improve the solubility (Chieng et al., 2009; Graeser et al., 2009; Heinz et al., 2007; Patterson et al., 2007). For example, the low solubility (and thus bioavailability) of BCS II compounds can be enhanced by solid-state transformations, such as the conversion of crystalline forms of drugs to the amorphous form (Haleblian, 1975). Another interesting aspect of transforming crystalline drugs into amorphous drugs is that the higher solubility often correlates with a faster dissolution rate of the drug (Karmwar et al., 2011b; Savolainen et al., 2009). The dissolution rate is also critical for the application of a drug, since adsorption via the oral route is only possible during gastro-intestinal passage of the drug. Examples of drugs for which the transformation into amorphous solids has improved their applicability in pharmaceutical industry, include indomethacin (Imaizumi et al., 1980), carbamazepine (Seefeldt et al., 2007), dipyridamole (Patterson et al., 2007), novobiocin (Mullin, 1961), itraconazole (Jung et al., 1999) and celecoxib (Gupta et al., 2004).

However, the amorphous form of drugs also encounters a major drawback: due to their high levels of energy (disorder), they are also inherently unstable, both physically and chemically. This is

* Corresponding author. Tel.: +49 7351 54 141973; fax: +49 7351 83 141972.
E-mail address: pranav.karmwar@boehringer-ingelheim.com (P. Karmwar).

0928-0987/$ - see front matter © 2013 Elsevier B.V. All rights reserved.
http://dx.doi.org/10.1016/j.ejps.2013.05.003

the reason, why traditionally crystalline forms of drugs are preferred in pharmaceutical formulations (Craig et al., 1999).

The physical stability of amorphous active pharmaceutical ingredient (API) can be increased by the use of miscible polymers. There has been much debate in the pharmaceutical literature about mechanisms involved in the physical stabilization of amorphous systems (Chieng et al., 2009; Karmwar et al., 2011a; Patterson et al., 2008; Sethia and Squillante, 2004; Taylor and Zografi, 1997; Van den Mooter et al., 2001). The formulation approach using drug–polymer blends has been used in the past in order to inhibit the crystallisation of the API in amorphous solid dispersions than the amorphous API alone. The aggregation/agglomeration of individual drug particles exhibiting a high solid–liquid surface tension is prevented by the presence of the carrier and it also creates a microenvironment, where the solubility of the drug is higher as compared to their crystalline counterparts (Six et al., 2004). The vast majority of drugs contain hydrogen-bonding sites. The presence or absence of intermolecular hydrogen bonds greatly influence properties such as cohesion and mixing of powders, adhesion and wetting (Castellanos, 2005; Li et al., 2011; Narang and Srivastava, 2002).

Drug–polymer systems (amorphous solid dispersions) lead to a promising approach for improving the oral bioavailability of poor water-soluble drugs, where a hydrophobic drug is dispersed within an inert matrix. Understanding the drug–polymer systems is of utmost significance to facilitate the optimisation of such formulations on the basis of structural variations, physical stability and dissolution. Trial and error experiments govern the screening process of polymeric excipients used in pharmaceutical formulations, with no systematic method available till date, to select a suitable functional polymer. The physicochemical properties of API are by large the major concern in the selection of a suitable polymer for solid dispersions. Whilst studies evaluating interaction affinity of API with individual polymers and the effect drug–polymer ratio on stability and dissolution have been conducted in the past (Chee, 1995; Marsac et al., 2009; Meaurio et al., 2005; Park et al., 2005; Vanhee et al., 2000), there has been comparatively little research into understanding the effect of drug–polymer interaction on the release of API from polymer matrix along with the degree of supersaturation as a function of time.

From a pharmaceutical industry perspective, the drug–polymer interaction governs the formulation selection for different stages of drug development. The formulation optimisation for early stage drug development is mainly C_{max} (concentration maximum) driven whereas the formulation for toxicological studies is *AUC* (area under the curve) driven.

The aim of this study was to investigate whether amorphous solid dispersions of telmisartan samples prepared (melt quenching) using different polymers, exhibit different structural characteristics (investigated by X-ray diffraction and Raman spectroscopy) along with different interaction affinity (calculated from differential scanning calorimetry measurements using the Flory–Huggins theory) and physical stability (time to crystallisation) and whether these can be correlated to the dissolution behaviour of the amorphous solid dispersions.

Telmisartan is an orally active, nonpeptide angiotensin II receptor antagonist. The renin–angiotensin system (RAS) plays an important role in the control of blood pressure and the regulation of volume and electrolyte homeostasis. It has a long duration of action and has the longest half-life of any angiotensin receptor blocker (Aoki et al., 2010; Kang et al., 1994; Ogihara et al., 1993). Since telmisartan is so effective, usage is increasing relative to those of other hypertension treatments. According to the biopharmaceutic classification system (BCS) (Löbenberg and Amidon, 2000), telmisartan is a class II drug with a log*P* value of 7.23, p*Ka* value of 3.5, 4 and 5.6 and poor water solubility of ≈1 μg ml^{-1}; however, it is freely soluble in highly alkalized solution. Telmisartan is a substituted benzimidazole derivative (Fig. 1). It has been proposed to have up to three different forms (two anhydrous forms, A and B, and a solvated form, C) (Dinnebier et al., 2000). The drug is marketed under the trade names Pritor™ and Micardis®.

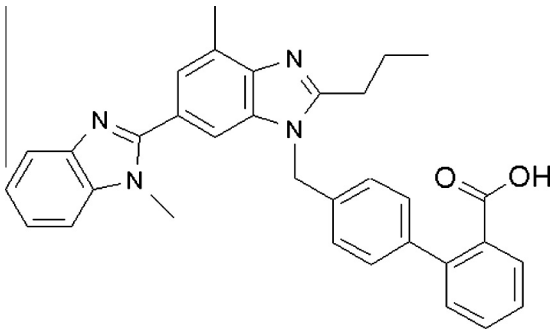

Fig. 1. Molecular structure of telmisartan.

2. Materials and methods

2.1. Materials

Telmisartan (>99% purity, form A) was synthesized in-house (Boehringer-Ingelheim Pharma, Germany). Soluplus and polyvinylpyrrolidone (PVP) K25 were obtained from BASF (Ludwigshafen, Germany), Hydroxypropyl methylcellulose (HPMC) E5 from Colorcon, Inc. (Pennsylvania, USA) and Eudragit E100 from Evonik industries (Krefeld, Germany). All materials were used as received.

2.2. Preparation of physical mixtures, amorphous samples and amorphous solid dispersions

2.2.1. Physical mixture

The drug and polymers were ground and sieved (separately) to obtain particles in the range 50–100 μm. Physical mixture of drug and polymer (7:3) was prepared using an oscillatory ball mill (Mixer Mill MM301, Retsch GmbH & Co., Haan, Germany). The powder sample was placed in 4 ml volume glass milling jar containing two 4 mm diameter glass beads. The samples were milled at 22 ± 2 °C with a frequency of 15 Hz for up to 2 min. Samples were prepared in triplicate.

2.2.2. Amorphous drug and amorphous solid dispersions

Telmisartan (form A) and physical mixtures thereof were melted in an aluminium cup at 275 °C and then cooled immediately using liquid nitrogen. The resulting amorphous solid was then warmed to room temperature over silica gel and then grounded and seived to obtain particles in the range of 50–100 μm. No chemical decomposition of telmisartan was observed for any of the samples in HPLC analysis. Samples were prepared in triplicate.

Amorphous telmisartan (pure drug) and amorphous solid dispersions (ASDs) of telmisartan will be referred to as amorphous samples and ASD of telmisartan with eudragit, soluplus, HPMC and PVP will be referred to as ASD of eudragit, soluplus, HPMC and PVP respectively in this manuscript.

2.2.3. Storage

A suspension of 100 mg ml^{-1} (equivalent to 70 mg ml^{-1} telmisartan) for all the freshly prepared amorphous samples was prepared (0.1 M McIlvaine buffer pH 4) and stored at room temperature (20 ± 1 °C) under continuous stirring until the onset of crystallisation was detected. The suspensions were collected

after predefined time points and filled in a glass capillary which was then mounted in X-ray instrument for detecting the onset of crystallisation.

2.3. Characterisation

The freshly prepared and stored samples were characterised using the following techniques. The freshly prepared samples were analysed within 1 h of preparation.

2.3.1. X-ray powder diffraction (XRPD)

The samples were analysed using XRPD with a STOE Stadi P system (STOE, Darmstadt, Germany) using Cu Kα radiation with λ = 1.5406 Å and a divergence slit of 1°. The samples were filled in a glass capillary and scanned at 40 kV and 40 mA from 3°2θ to 25°2θ using a scanning speed of 0.1285° min^{-1} and a step size of 0.006°. The diffraction patterns were generated using WinXPOW version 3.0.1.13 (STOE, Darmstadt, Germany).

2.3.2. Raman spectroscopy

The Raman spectrophotometer consisted of a LabRam HR (Horiba Jobin Yvon Raman division, Bensheim, Germany). The analysis was carried out at room temperature utilising a laser wavelength of 632 nm (HeNe laser). Spectra were the average of 64 scans, taken at 4 cm^{-1} resolution with a laser power of 120 mW. The spectra were generated using LabSpec version 5.64.15 (Horiba Jobin Yvon Raman division, Bensheim, Germany).

Principal components analysis (PCA) was used to help interpret differences in the XRPD diffractograms and Raman spectra of the different amorphous samples. Before PCA, normalisation was performed on the spectra to remove intensity differences unrelated to the sample composition and the spectra were then mean centred. PCA was performed on 3°2θ–25°2θ and 1000 cm^{-1} to 1750 cm^{-1} for the X-ray diffractograms and Raman spectra respectively. PCA, spectral preprocessing and scaling were performed using The Unscrambler software version 10.2 (CAMO Software AS, Oslo, Norway).

2.3.3. Differential scanning calorimetry (DSC)

DSC thermograms were recorded on a DSC Q2000 calorimeter version 24.8.120 (TA Instruments, New Castle, USA) after temperature and enthalpy calibration using indium. Samples (2–5 mg) were crimped in an aluminium pan and heated at a rate of 10 K min^{-1} from 0 to 275 °C under a nitrogen gas flow of 50 ml min^{-1}. The glass transition temperature (T_g), crystallisation temperature (T_c) and melting temperature (T_m) were determined using TA Universal Analysis software (version 4.3A). The T_g was defined as the midpoint of the change in heat capacity of the sample, while T_m for the crystalline drug and physical mixtures were defined using the offset temperatures. The offset of melting temperature for all the physical mixtures was considered as the melting point depression and was used in estimating Flory–Huggins interaction parameter. The depression in the melting point of drug–polymer mixture can be used for the estimation of Flory–Huggins interaction parameter (χ) (Marsac et al., 2006). The relationship between the melting point depression and interaction parameter (χ) can be mathematically expressed as (Marsac et al., 2009):

$$\left(\frac{1}{T_M^{mix}}-\frac{1}{T_M^{pure}}\right)=\frac{-R}{\Delta H_{fus}}\left[\ln\phi_{drug}+\left(1-\frac{1}{m}\right)\phi_{polymer}+\chi\phi_{ploymer}^2\right] \quad (1)$$

Here, T_M^{mix} is the depressed melting point of the physical mixture, T_M^{pure} is the melting point of the pure drug, R is the gas constant, ΔH_{fus} is the heat of fusion of the pure drug, m is molar volume ratio of polymer and drug, χ is Flory–Huggins interaction parameter, ϕ_{drug} and $\phi_{polymer}$ are weight fraction of drug and polymer respectively.

Analysis of variance (ANOVA) was performed on the thermal events and Flory–Huggins interaction parameter for all the samples using Microsoft Excel (Microsoft Corporation, Washington, USA).

2.3.4. Dissolution studies

All the dissolution experiments were performed in µDISS Profiler™ version 4.2.0.21 (*p*ION INC, Massachusetts, USA) coupled with a fibre optic detection system. Samples were continuously analysed for telmisartan concentration using a dipped UV probe in the dissolution media at a wavelength of 297 nm. Samples (equivalent to 5 mg of telmisartan) were placed in the dissolution medium and the dissolution rate was determined at 37 ± 0.2 °C in 10 ml of 0.1 M McIlvaine buffer pH 4 at 400 rpm. All measurements were carried out in triplicate. Analysis of variance (ANOVA) was performed on the *AUC* of the dissolution profile and C_{max} values for all the different amorphous samples using Microsoft Excel (Microsoft Corporation, Washington, USA).

3. Results and discussion

3.1. Freshly prepared samples

3.1.1. XRPD

Complete absence of diffraction peaks in the diffractograms of all freshly prepared amorphous samples revealed that telmisartan was completely "X-ray amorphous" (Fig. 2). However, the shape of these diffractograms varied, suggesting structural variations in the near order of the molecules between the different amorphous samples. All samples, except ASD of eudragit and amorphous telmisartan, featured relatively broad maxima in the halos. The diffractograms of all the samples had relatively intense maxima at approximately 7°2θ, and much a weaker feature centred around 17°2θ. The two maxima for ASD of eudragit and amorphous telmisartan in the diffractograms were of similar shape and position, but slightly different intensity. These data were reproducible for the three batches for each ASD (only one diffractogram is shown in Fig. 2 for all amorphous samples). Raman spectroscopy was performed on the same samples to help understand the nature of the structural differences between the samples.

3.1.2. Raman spectroscopy

Raman spectroscopy was performed on the same samples as in the XRPD study with the purpose of investigating structural differences between the samples. The Raman spectra of all the freshly prepared amorphous samples contained peaks that were broader and more merged than those of the crystalline forms (Fig. 3a), which is due to the inherently larger variations in molecular conformation and intermolecular bonding of amorphous forms compared to their crystalline counterparts (Savolainen et al., 2007; Strachan et al., 2007). There peak position differences between the amorphous and crystalline forms were observed at 1285 cm^{-1}, 1453 cm^{-1}, 1530 cm^{-1} and 1618 cm^{-1}. However, there were no spectral features specific to telmisartan form A for any of the amorphous samples.

Spectral variation between the different amorphous samples was investigated by performing PCA. Three principal components (PCs) explained 96% of the variation in the normalised and centred data. The relationship between the different samples was investigated using the scores plot (Fig. 3b), based on the PCA model. The spectra of all the freshly prepared amorphous samples prepared in triplicate clustered in the scores plot, suggesting that structural differences due to different polymers are reproducible.

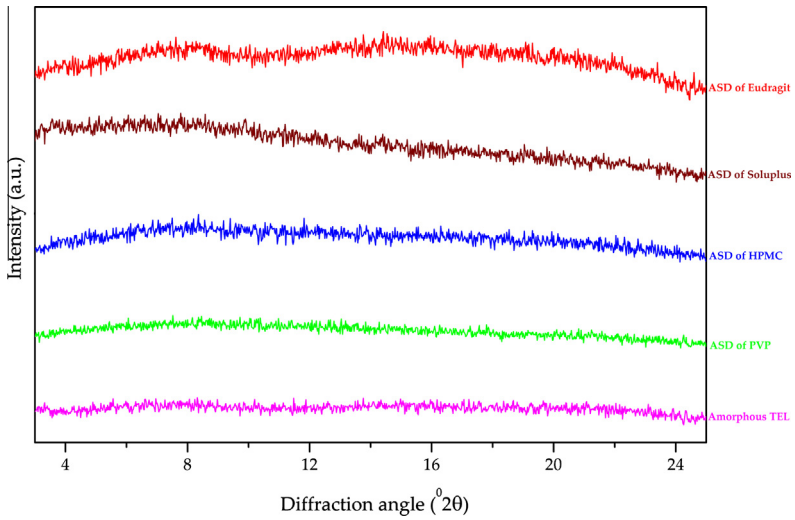

Fig. 2. Diffractograms of freshly prepared amorphous samples of telmisartan prepared by melt quenching technique.

It can be observed that the samples clustered in the scores plot on the basis of polymers used. In the scores plot, ASD of eudragit and soluplus formed its own cluster whereas ASD of HPMC and PVP positioned close to each other and formed one cluster. The pure amorphous sample formed a separate cluster. The clusters observed in the scores plot does not mirror the differences observed in the diffractograms of the amorphous samples (Fig. 1).

The spectral loadings plots (Fig. 3c) were used in an attempt to interpret sample differences leading to the clustering observed in the scores plot. The loadings of the three PCs revealed that the largest spectral differences were observed in the regions from 1280 cm^{-1} to 1620 cm^{-1}. The main vibrations associated with the bands in these regions can be assigned for amorphous telmisartan as follows: acyclic CC chain vibrations (1285 cm^{-1}), asymmetric CH_2 and CH_3 vibrations (1453 cm^{-1}), benzimidazole ring deformation (1530 cm^{-1}) and benzimidazole C=N stretching (1618 cm^{-1}). The range of vibrations associated with the largest spectral differences suggests that the systematic differences associated with the different solid dispersions prepared were due to a range of molecular conformations and intermolecular interactions, and cannot be attributed to one or a few vibrations only.

3.1.3. Thermal analysis

For all freshly prepared amorphous samples, the DSC thermograms exhibited a change in heat capacity (ΔC_p) in the range of 85–140 °C (Table 1). An exothermic and endotherm event was found for the pure amorphous telmisartan around 201 ± 1.6 °C and 272 ± 0.1 °C respectively (Table 1). A small exothermic and endothermic event was observed for ASD of HPMC and PVP ≈205 °C and ≈268 °C respectively. In contrast, ASD of eudragit and soluplus showed no exothermic or endothermic event (Table 1). The change in heat capacity can be attributed to the T_g of the sample and T_c was associated with recrystallisation of amorphous telmisartan. The endotherm around 270 °C was due to melting of form A of telmisartan.

A statistical significance was observed in the melting point depression for all the physical mixtures (Table 2). The systems which exemplify a depression in the melting point have been identified as miscible whereas immiscible or partially miscible systems shows no depression in the melting point of the drug (Shamblin et al., 1998; Van den Mooter et al., 2001; Yoshioka et al., 1995). The chemical potential of the crystalline and molten drug is equal at the melting temperature of the pure drug. If miscibility persists between the drug and polymer, then the chemical potential of the pure drug is higher than the chemical potential of the mixture (Cesteros et al., 1993; Flory, 1953; Marsac et al., 2009,2006). The negative values of the interaction parameter values are resulting due to higher melting point depression and suggest exothermic mixing whereas positive interaction values results due to lower melting point depression and entail the involvement of endothermic mixing. Immiscible systems are expected to show no melting point depression and consequently exhibiting positive interaction values (Cesteros et al., 1993; Flory, 1953; Marsac et al., 2009,2006; Nishi and Wang, 1975). In this study, telmisartan showed varying degrees of melting point depression when mixed with eudragit, soluplus, HPMC and PVP. The depression in the melting point of telmisartan was highest with eudragit followed by soluplus, HPMC and PVP (Table 2). The highest interaction between telmisartan and eudragit mixture can be attributed to the counter-ionic interaction of weak acidic drug (telmisartan) and ionic polymer (eudragit E100) (Sarode et al., 2013).

ANOVA analysis was performed on the T_g and associated ΔC_p and on χ. Statistical significance was observed for T_g and ΔC_p, for all the amorphous samples prepared with/without polymers (p-value < 0.01). The difference in the T_g and ΔC_p of the samples can be ascribed to the differences in the amorphous state (Karmwar et al., 2011a). The ASD of eudragit showed the lowest T_g, followed by soluplus, HPMC and PVP samples. Statistical significance was also obtained for χ for all the physical mixtures of telmisartan used in this study (p-value < 0.01).

3.2. Dissolution studies

The dissolution experiments were performed under non-sink conditions to investigate the concentration–time profile, C_{max} and *AUC* of different amorphous samples of telmisartan when exposed to the dissolution medium. The calculation of *AUC* was performed on the basis of 60 h of dissolution studies. For comparison, dissolution studies (pH 4) were performed with physical mixtures of telmisartan and polymers to clarify the solubilising potency of co-existing polymers. The telmisartan concentrations from the physical mixtures (≈7 μg ml^{-1}) were slightly higher than the crystalline telmisartan (≈1 μg ml^{-1}) and significantly lower than the ASD (p-value < 0.01) (data not shown). This suggests that the higher dissolution behaviour of ASD was due the drug–polymer interaction and not due to the solubilising effect of the polymers used.

A significant difference was observed in C_{max} and *AUC* of crystalline and amorphous telmisartan (p-value < 0.01). Amorphous

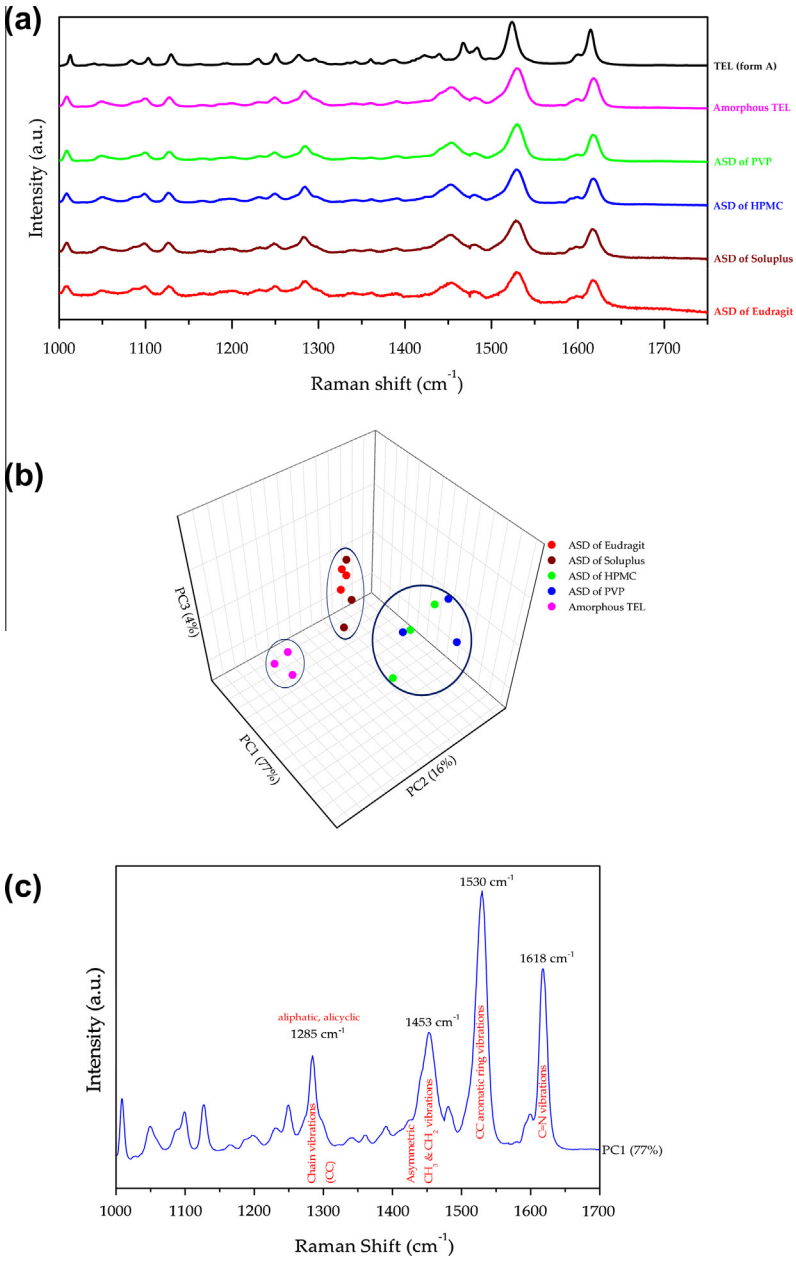

Fig. 3. Raman spectra (a); scores plot (b); and their corresponding loadings (c) of all freshly prepared amorphous samples of telmisartan.

Table 1
Thermal properties of amorphous samples of telmisartan prepared by melt quenching technique (mean ± SD, n = 3).

Amorphous samples	T_g (°C)	ΔC_p (J/(g °C))	T_c (°C)	T_m (°C)
Telmisartan	135.4 ± 0.97	0.44 ± 0.08	201 ± 1.26	272.3 ± 0.15
ASD of eudragit	87.8 ± 0.22	0.23 ± 0.01	–	–
ASD of soluplus	115.9 ± 0.56	0.40 ± 0.01	–	–
ASD of HPMC	132.7 ± 0.22	0.44 ± 0.07	202.2 ± 2.44	268.3 ± 0.86
ASD of PVP	139.2 ± 0.92	0.41 ± 0.01	204.1 ± 1.68	268.4 ± 1.30

Table 2
Interaction parameter and offset of melting values for all the physical mixtures of telmisartan.

Physical mixtures	Offset of melting (°C)	Interaction parameter (χ)
ASD of eudragit	260.8 ± 0.64	−0.61
ASD of soluplus	268.7 ± 0.10	−0.63
ASD of HPMC	271.0 ± 0.11	−0.66
ASD of PVP	272.1 ± 0.30	−0.67

telmisartan and ASD of HPMC and PVP samples showed a very fast dissolution and attain C_{max} within 5 min. A significant difference was observed in C_{max} and *AUC* for amorphous telmisartan and ASD of HPMC and PVP (p-value < 0.01) whereas no statistical difference was found for T_{max} (p-value > 0.01). A slow dissolution was observed for ASD of eudragit and soluplus and no statistical significance for C_{max}, T_{max} and *AUC* was observed (p-value > 0.01) for these samples (Fig. 4). Amorphous telmisartan showed C_{max} of ≈44 μg ml^{-1} and maintained supersaturation for ≈1 h whereas ASD of PVP showed C_{max} of ≈113 μg ml^{-1} and maintained supersaturation for ≈20 h while ASD of eudragit, soluplus and HPMC showed C_{max} of ≈87, ≈89 and ≈136 μg ml^{-1} respectively and did not showed any precipitation during the experimental time scale

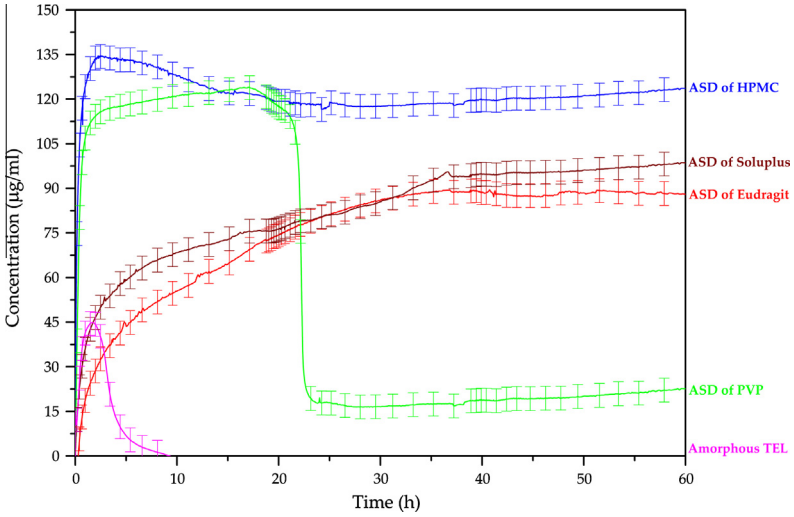

Fig. 4. Dissolution profiles of all amorphous samples of telmisartan at 37 ± 0.2 °C.

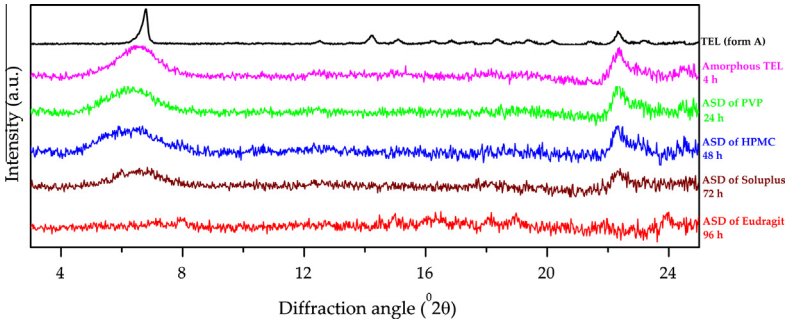

Fig. 5. Diffractograms showing the onset of crystallisation for different amorphous suspensions of telmisartan.

(i.e. 60 h) of dissolution studies (Fig. 4). The total amount of telmisartan in solution after 120 min was ≈25–140 times higher for all amorphous samples as compared to telmisartan form A, whilst the amount of telmisartan in solution after 120 min was ≈3 times and ≈4 times higher for the ASD of PVP and HPMC compared to amorphous telmisartan. The increase in C_{max} and *AUC* for ASD may be an indicator that different polymers interact differently, affecting the physical stability and re-crystallisation kinetics of the disordered solids and further enhancing the dissolution (Bøtker et al., 2011; Karmwar et al., 2012).

Since fibre optic UV probes were used in order to determine the concentration of telmisartan, the apparent supersaturation can be attributed to various sub-micron particulate species (Sarode et al., 2013). In order to ascertain that the precipitated particles do not interfere or influence the supersaturation levels attained by the ASD, particle size analysis (Horiba nanoparticle analyser SZ 100) was performed on the precipitated samples. The particles were bigger than 8 µm (data not shown) and the sedimentation of these particles can be envisioned by naked eye. Hence, suggesting that supersaturation attained was characteristic of the molecularly dissolved telmisartan (Alonzo et al., 2011; Sarode et al., 2013).

3.3. Recrystallisation

X-ray diffraction was used to determine the time to onset of crystallisation of the drug (Fig. 5). The time to onset of crystallisation was defined as the time until diffraction peaks were visible in the diffractograms. The time to onset of crystallisation is shown for all amorphous samples in Table 3. The XRD diffractogram scores plot also revealed the movement of the stored samples away from the cluster of freshly prepared amorphous samples towards the crystalline or semi-crystalline samples (amorphous:crystalline (1:1) physical mixture), as a function of time and polymers used (Fig. 6). The ranking of the amorphous samples with respect to stability was: ASD of eudragit > ASD of soluplus > ASD of HPMC > ASD of PVP > amorphous telmisartan. This ranking can be correlated with sample distribution in the scores plot of the Raman spectra (Fig. 3b). The most stable, moderately stable and the least stable samples formed their own cluster in the scores plot, suggesting that the time until onset of crystallisation was affected by structural variation in the samples but could not be correlated with the diffractogram shapes.

Table 3
Onset of crystallisation for amorphous suspensions of telmisartan.

Amorphous samples	Onset of crystallisation (h)
Telmisartan	4 ± 2
ASD of eudragit	96 ± 8
ASD of soluplus	72 ± 5
ASD of HPMC	48 ± 6
ASD of PVP	24 ± 5

Upon storage, all quench cooled samples in which the starting polymorph can be assumed to have no effect on the crystallisation behaviour (since the drug passes through a melt state), crystallised to polymorph A. Interestingly, the clustering of the spectra (freshly

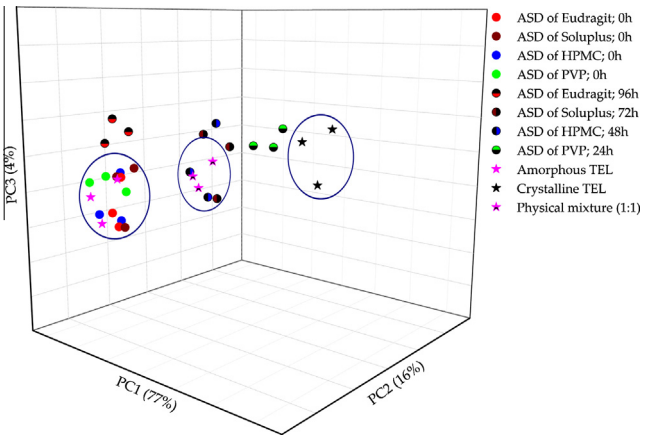

Fig. 6. PCA scores plot of the XRD diffractogram of all freshly prepared amorphous samples and stored samples (onset of crystallisation) of telmisartan.

prepared samples) in the PCA scores plot can be linked to the structural variations but cannot be correlated with the physical stability. However, it can be speculated that structural differences in the different solid dispersions based on scores plot, may have an influence on physical stability.

3.4. Comparison of interaction parameter, physical stability and dissolution behaviour

The calculated values for the interaction parameter and T_g obtained from the DSC thermograms were compared to the experimental physical stability of the amorphous systems. It was observed that the interaction parameter values calculated using Flory–Huggins theory was in good agreement with the physical stability for all the ASD. An amorphous system with high interaction parameter values illustrate less interaction between drug and polymer and should recrystallise the fastest (Ivanisevic, 2010; Marsac et al., 2006; Shamblin et al., 1998). The correlation

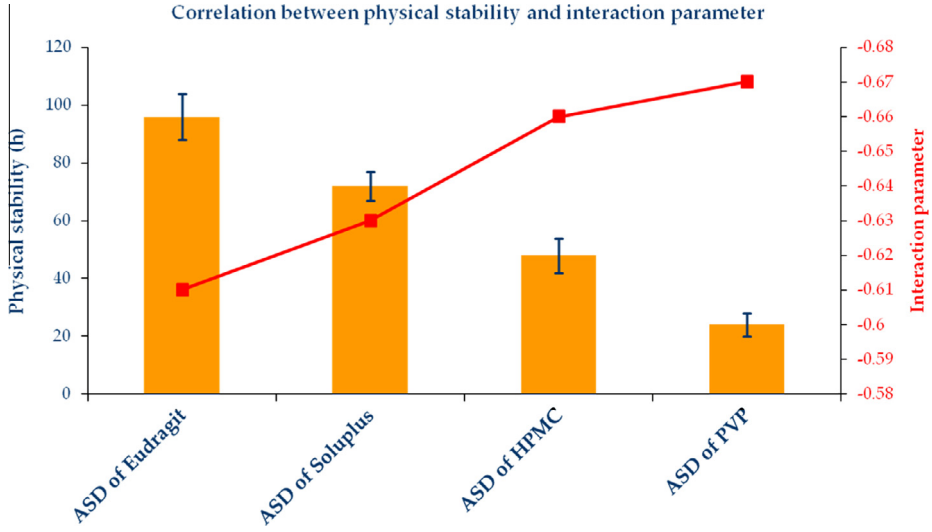

Fig. 7. Correlation of interaction parameter (χ) with the experimentally determined stability (onset of crystallisation) for different ASD of telmisartan.

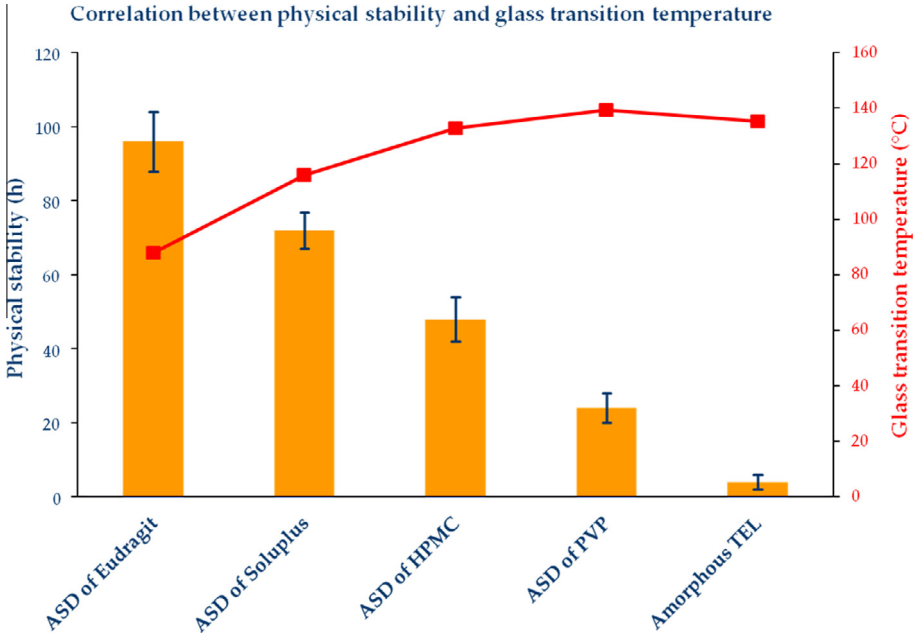

Fig. 8. Correlation of and glass transition temperature (T_g) with the experimentally determined stability (onset of crystallisation) for different amorphous samples of telmisartan.

of interaction parameter (χ) and physical stability (onset of crystallisation) can be seen in Fig. 7. The order of physical stability and interaction parameter (χ) was the same: ASD of eudragit > ASD of soluplus > ASD of HPMC > ASD of PVP.

The T_g for all the amorphous samples were recorded from dry solid powder and are listed in Table 1. There was no correlation obtained between the T_g (dry powders) and physical stability (suspensions) (Fig. 8). The absence of any correlation between T_g and physical stability can be attributed to (i) plasticising effect of water varies from polymer to polymer, (ii) the drug–polymer interaction affinity, (iii) moisture sorption differences of polymers (He et al., 2004; Nishi and Wang, 1975; Tian et al., 2012; Wiranidchapong et al., 2008). The T_g of pure amorphous telmisartan is higher than the ASD of telmisartan, hence in this case the polymers are acting as a plasticiser for telmisartan. With these prerequisites it can be considered challenging to correlate the T_g (dry powder) with the physical stability (suspension).

The dissolution profile showed a good correlation with interaction parameter and physical stability of all amorphous samples. The dissolution behaviour for all ASD (except ASD of HPMC) was inversely proportional to the interaction parameter; higher the C_{max}, less the interaction between the drug and polymer and vice versa. In contrast, the *AUC* was directly proportional to the physical stability of all amorphous samples (except ASD of HPMC); higher the physical stability, longer the time for crystallisation. Dissolution behaviour of ASD of HPMC does not showed any correlation with the physical stability and interaction parameter can be attributed to (i) semicrystalline morphology of HPMC, (ii) HPMC has been shown to prevent recrystallisation and thus prolonging supersaturation in a wide variety of formulations (Usui et al., 1997), (iii) HPMC is also described as a 'spacer' between drug molecules or drug particles or it was used as a surface coating on amorphous drug particles (Matteucci et al., 2007). It can be further speculated that the dissolution behaviour of ASD of HPMC is influenced by the resulting viscosity of the dissolution media and also due to some interaction which was not detected by Raman spectroscopy. It is therefore of interest to further investigate and get a better understanding of drug–polymer interaction using solid state NMR.

This suggests that structural differences in the different amorphous samples may influence the dissolution behaviour, interaction parameter and physical stability, which to some extent is reflected on the basis of clustering in the Raman spectra scores plot (Fig. 3b).

4. Conclusion

In this study it was demonstrated that different amorphous samples of the drug telmisartan showed differences on the molecular level (detected by Raman spectroscopy and XRD). These differences however, could not be correlated directly to the physical stability of the samples. However, there was some evidence that the molecular level variation influenced the thermal properties, dissolution behaviour and physical stability.

This study has also shown that the interaction parameter – determined by the Flory–Huggins theory – could be used to rank the same amorphous systems prepared using different polymers correctly according to their dissolution behaviour and physical stability. The presence of polymers has a significant impact on the dissolution behaviour and physical stability of ASD.

The different stages of drug development need different dissolution behaviour. Early stage drug development needs higher C_{max} whereas in later stage (toxicological studies) higher *AUC* is required. Hence, this information may help the formulation scientist to select an appropriate polymer for different stages of drug development.

References

Alonzo, D.E., Gao, Y., Zhou, D., Mo, H., Zhang, G.G.Z., Taylor, L.S., 2011. Dissolution and precipitation behavior of amorphous solid dispersions. J. Pharm. Sci. 100, 3316–3331.

Aoki, A., Ogawa, T., Sumino, H., Kumakura, H., Takayama, Y., Ichikawa, S., Nitta, K., 2010. Long-term effects of telmisartan on blood pressure, the renin–angiotensin–aldosterone system, and lipids in hypertensive patients. Heart Vessels 25, 195–202.

Bøtker, J.P., Karmwar, P., Strachan, C.J., Cornett, C., Tian, F., Zujovic, Z., Rantanen, J., Rades, T., 2011. Assessment of crystalline disorder in cryo-milled samples of indomethacin using atomic pair-wise distribution functions. Int. J. Pharm. 417, 112–119.

Castellanos, A., 2005. The relationship between attractive interparticle forces and bulk behaviour in dry and uncharged fine powders. Adv. Phys. 54, 263–376.

Cesteros, L.C., Meaurio, E., Katime, I., 1993. Miscibility and specific interactions in blends of poly(hydroxy methacrylates) with poly(vinylpyridines). Macromolecules 26, 2323–2330.

Chee, K.K., 1995. Thermodynamic study of glass transitions in miscible polymer blends. Polymer 36, 809–813.

Chieng, N., Aaltonen, J., Saville, D., Rades, T., 2009. Physical characterization and stability of amorphous indomethacin and ranitidine hydrochloride binary systems prepared by mechanical activation. Eur. J. Pharm. Biopharm. 71, 47–54.

Craig, D.Q.M., Royall, P.G., Kett, V.L., Hopton, M.L., 1999. The relevance of the amorphous state to pharmaceutical dosage forms: glassy drugs and freeze dried systems. Int. J. Pharm. 179, 179–207.

Dinnebier, R.E., Sieger, P., Nar, H., Shankland, K., David, W.I.F., 2000. Structural characterization of three crystalline modifications of telmisartan by single crystal and high-resolution X-ray powder diffraction. J. Pharm. Sci. 89, 1465–1479.

Flory, P.J., 1953. Principles of Polymer Chemistry. Cornell University Press, Ithaca.

Graeser, K.A., Patterson, J.E., Rades, T., 2009. Applying thermodynamic and kinetic parameters to predict the physical stability of two differently prepared amorphous forms of simvastatin. Curr. Drug Deliv. 6, 374–382.

Gupta, P., Kakumanu, V.K., Bansal, A.K., 2004. Stability and solubility of celecoxib-PVP amorphous dispersions: a molecular perspective. Pharm. Res. 21, 1762–1769.

Haleblian, J.K., 1975. Characterization of habits and crystalline modification of solids and their pharmaceutical applications. J. Pharm. Sci. 64, 1269–1288.

He, Y., Zhu, B., Inoue, Y., 2004. Hydrogen bonds in polymer blends. Prog. Polym. Sci. 29, 1021–1051.

Heinz, A., Savolainen, M., Rades, T., Strachan, C.J., 2007. Quantifying ternary mixtures of different solid-state forms of indomethacin by Raman and near-infrared spectroscopy. Eur. J. Pharm. Sci. 32, 182–192.

Imaizumi, H., Nambu, N., Nagai, T., 1980. Pharmaceutical interaction in dosage forms and processing (18). Stability and several physical-properties of amorphous and crystalline forms of indomethacin. Chem. Pharm. Bull. 28, 2565–2569.

Ivanisevic, I., 2010. Physical stability studies of miscible amorphous solid dispersions. J. Pharm. Sci. 99, 4005–4012.

Jung, J.-Y., Yoo, S.D., Lee, S.-H., Kim, K.-H., Yoon, D.-S., Lee, K.-H., 1999. Enhanced solubility and dissolution rate of itraconazole by a solid dispersion technique. Int. J. Pharm. 187, 209–218.

Kang, P.M., Landau, A.J., Eberhardt, R.T., Frishman, W.H., 1994. Angiotensin II receptor antagonists: a new approach to blockade of the renin–angiotensin system. Am. Heart J. 127, 1388–1401.

Karmwar, P., Boetker, J.P., Graeser, K.A., Strachan, C.J., Rantanen, J., Rades, T., 2011a. Investigations on the effect of different cooling rates on the stability of amorphous indomethacin. Eur. J. Pharm. Sci. 44, 341–350.

Karmwar, P., Graeser, K., Gordon, K.C., Strachan, C.J., Rades, T., 2011b. Investigation of properties and recrystallisation behaviour of amorphous indomethacin samples prepared by different methods. Int. J. Pharm. 417, 94–100.

Karmwar, P., Graeser, K., Gordon, K.C., Strachan, C.J., Rades, T., 2012. Effect of different preparation methods on the dissolution behaviour of amorphous indomethacin. Eur. J. Pharm. Biopharm. 80, 459–464.

Li, B., Wen, M., Li, W., He, M., Yang, X., Li, S., 2011. Preparation and characterization of baicalin-poly-vinylpyrrolidone coprecipitate. Int. J. Pharm. 408, 91–96.

Löbenberg, R., Amidon, G.L., 2000. Modern bioavailability, bioequivalence and biopharmaceutics classification system. New scientific approaches to international regulatory standards. Eur. J. Pharm. Biopharm. 50, 3–12.

Marsac, P., Shamblin, S., Taylor, L., 2006. Theoretical and practical approaches for prediction of drug–polymer miscibility and solubility. Pharm. Res. 23, 2417–2426.

Marsac, P., Li, T., Taylor, L., 2009. Estimation of drug–polymer miscibility and solubility in amorphous solid dispersions using experimentally determined interaction parameters. Pharm. Res. 26, 139–151.

Matteucci, M.E., Brettmann, B.K., Rogers, T.L., Elder, E.J., Williams, R.O., Johnston, K.P., 2007. Design of potent amorphous drug nanoparticles for rapid generation of highly supersaturated media. Mol. Pharm. 4, 782–793.

Meaurio, E., Zuza, E., Sarasua, J.-R., 2005. Miscibility and specific interactions in blends of poly(l-lactide) with poly(vinylphenol). Macromolecules 38, 1207–1215.

Mullin, J.W., 1961. Crystallization. International Scientific Series, Butterworths, London.
Narang, A.S., Srivastava, A.K., 2002. Evaluation of solid dispersions of clofazimine. Drug Dev. Ind. Pharm. 28, 1001–1013.
Nishi, T., Wang, T.T., 1975. Melting point depression and kinetic effects of cooling on crystallization in poly(vinylidene fluoride)-poly(methyl methacrylate) mixtures. Macromolecules 8, 909–915.
Ogihara, T., Higashimori, K., Masuo, K., Mikami, H., 1993. Pilot study of a new angiotensin II receptor antagonist, TCV-116: effects of a single oral dose on blood pressure in patients with essential hypertension. Clin. Ther. 15, 684–691.
Park, Y., Veytsman, B., Coleman, M., Painter, P., 2005. The miscibility of hydrogen-bonded polymer blends: two self-associating polymers. Macromolecules 38, 3703–3707.
Patterson, J.E., James, M.B., Forster, A.H., Lancaster, R.W., Butler, J.M., Rades, T., 2007. Preparation of glass solutions of three poorly water soluble drugs by spray drying, melt extrusion and ball milling. Int. J. Pharm. 336, 22–34.
Patterson, J.E., James, M.B., Forster, A.H., Rades, T., 2008. Melt extrusion and spray drying of carbamazepine and dipyridamole with polyvinylpyrrolidone/vinyl acetate copolymers. Drug Develop. Ind. Pharm. 34, 95–106.
Sarode, A.L., Sandhu, H., Shah, N., Malick, W., Zia, H., 2013. Hot melt extrusion (HME) for amorphous solid dispersions: Predictive tools for processing and impact of drug–polymer interactions on supersaturation. Eur. J. Pharm. Sci. 48, 371–384.
Savolainen, M., Heinz, A., Strachan, C., Yliruusi, J., Rades, T., Sandler, N., 2007. Screening for differences in the amorphous state of indomethacin using multivariate visualization. Eur. J. Pharm. Sci. 32, S8.
Savolainen, M., Kogermann, K., Heinz, A., Aaltonen, J., Peltonen, L., Strachan, C., Yliruusi, J., 2009. Better understanding of dissolution behaviour of amorphous drugs by in situ solid-state analysis using Raman spectroscopy. Eur. J. Pharm. Biopharm. 71, 71–79.
Seefeldt, K., Miller, J., Alvarez-Núñez, F., Rodríguez-Hornedo, N., 2007. Crystallization pathways and kinetics of carbamazepine–nicotinamide cocrystals from the amorphous state by in situ thermomicroscopy, spectroscopy, and calorimetry studies. J. Pharm. Sci. 96, 1147–1158.
Sethia, S., Squillante, E., 2004. Solid dispersion of carbamazepine in PVP K30 by conventional solvent evaporation and supercritical methods. Int. J. Pharm. 272, 1–10.
Shamblin, S.L., Taylor, L.S., Zografi, G., 1998. Mixing behavior of colyophilized binary systems. J. Pharm. Sci. 87, 694–701.
Six, K., Verreck, G., Peeters, J., Brewster, M., Mooter, G.V.D., 2004. Increased physical stability and improved dissolution properties of itraconazole, a class II drug, by solid dispersions that combine fast- and slow-dissolving polymers. J. Pharm. Sci. 93, 124–131.
Strachan, C.J., Rades, T., Gordon, K.C., 2007. A theoretical and spectroscopic study of gamma-crystalline and amorphous indometacin. J. Pharm. Pharmacol. 59, 261–269.
Taylor, L.S., Zografi, G., 1997. Spectroscopic characterization of interactions between PVP and indomethacin in amorphous molecular dispersions. Pharm. Res. 14, 1691–1698.
Tian, Y., Jones, D.S., Li, S., Andrews, G.P., 2012. Construction of drug–polymer thermodynamic phase diagrams using flory–huggins interaction theory: identifying the relevance of temperature and drug weight fraction to phase separation within solid dispersions. Mol. Pharm..
Usui, F., Maeda, K., Kusai, A., Nishimura, K., Keiji, Y., 1997. Inhibitory effects of water-soluble polymers on precipitation of RS-8359. Int. J. Pharm. 154, 59–66.
Van den Mooter, G., Wuyts, M., Blaton, N., Busson, R., Grobet, P., Augustijns, P., Kinget, R., 2001. Physical stabilisation of amorphous ketoconazole in solid dispersions with polyvinylpyrrolidone K25. Eur. J. Pharm. Sci. 12, 261–269.
Vanhee, S., Koningsveld, R., Berghmans, H., Šolc, K., Stockmayer, W.H., 2000. Thermodynamic stability of immiscible polymer blends. Macromolecules 33, 3924–3931.
Wiranidchapong, C., Tucker, I.G., Rades, T., Kulvanich, P., 2008. Miscibility and interactions between 17β-estradiol and Eudragit® RS in solid dispersion. J. Pharm. Sci. 97, 4879–4888.
Yoshioka, M., Hancock, B.C., Zografi, G., 1995. Inhibition of indomethacin crystallization in poly(vinylpyrrolidone) coprecipitates. J. Pharm. Sci. 84, 983–986.